Influence of series resistance on the experimental extraction of FinFET noise parameters

Angeliki Tataridou, Gérard Ghibaudo, Christoforos Theodorou

Influence of series resistance on the experimental extraction of FinFET noise parameters

Angeliki Tataridou, Gerard Ghibaudo and Christoforos Theodorou
IMEP-LAHC
Univ. Grenoble Alpes, Univ. Savoie Mont Blanc, CNRS, Grenoble INP*
Grenoble, 38000, France
**Institute of Engineering Univ. Grenoble Alpes*
e-mail: angeliki.tataridou@grenoble-inp.fr

***Abstract*—In this paper we demonstrate for the first time how the series resistance of an advanced CMOS device, such as the FinFET, can lead to an incorrect extraction of low-frequency noise parameters. In particular, the use of the carrier number fluctuations with correlated mobility fluctuations model is shown to be very sensitive to the transistor series resistance. We demonstrate how the classic fitting methods can lead to an underestimated value in the extraction of the mobility fluctuations factor Ω. Furthermore, we present an original method for suppressing this effect, by taking advantage of the series resistance immune Y-function.**

I. INTRODUCTION

Low frequency noise (LFN) is attracting more and more interest in the last years, since it not only characterizes a device performance in terms of dynamic stability [1], but can also give significant information about the defects inside the oxide [2] or silicon [3] which is valuable especially in today's aggressively scaled devices like FinFETs [4], [5]. The utilization of LFN for the assessment of the oxide/silicon interface quality requires the reliable extraction of noise parameters such as the trap density, N_t, and the remote Coulomb scattering coefficient, α_{sc}.

This extraction is achieved using the well-established [6], [7], [8] carrier number fluctuations with correlated mobility fluctuations (CNF/CMF) model (1), which considers both the change of the flat-band voltage (V_{FB}) following the trapping/detrapping of free carriers and the mobility change due to the interface charge fluctuations [6].

$$\frac{S_{I_d}}{{I_d}^2} = \left(1 + \Omega \frac{I_d}{g_m}\right)^2 \left(\frac{g_m}{I_d}\right)^2 \ S_{V_{FB}} \tag{1}$$

S_{Vfb} is the flat-band voltage fluctuations power spectral density, and Ω is the CMF coefficient given by (2).

$$S_{V_{FB}} = \frac{q^2 \lambda k T N_t}{W L C_{ox}^2 f^{\gamma}} \ , \Omega = \alpha_{sc} \mu_{eff} C_{ox} \tag{2}$$

where, μ_{eff} is the effective mobility and C_{ox} the oxide capacitance per unit area, λ is the tunneling constant in the dielectric (≈ 0.1 nm), kT is the thermal voltage, q is the elementary charge of electrons, f the frequency, γ the characteristic exponent close to 1, N_t the volumetric trap density and W, L the channel width and length respectively.

This extraction is generally reliable in the case of long channel devices. However in short channel devices, the series resistance (R_{SD}) can degrade a FinFET's performance because it becomes important with respect to the reduced channel resistance. Therefore, the use of experimentally measured quantities such as the device extrinsic transconductance, g_m, for the noise parameter extraction through (1) may jeopardize the precision of the extraction procedure. In this work we study, for the first time, the impact of R_{SD} on the low-frequency noise (LFN) parameter extraction.

II. EXPERIMENTAL APPROACH AND DEVICE UNDER TEST

A very useful quantity in the LFN characterization and modeling is the input-referred gate voltage noise $S_{Vg} = S_{Id} / {g_m}^2$. It suppresses the impact of g_m on the measured noise and expresses every fluctuation as a gate voltage variation, which allows for easier model implementations in circuit simulations. Concerning its application in the extraction of LFN parameters, a method very often used by our team in recent works [7], [8] is to extract Ω from the slope of $\sqrt{S_{Vg}}$ vs I_d/g_m, thanks to the expression of (3):

$$\sqrt{S_{V_g}} = \sqrt{S_{V_{FB}}}\left(1 + \Omega \frac{I_d}{g_m}\right) \tag{3}$$

which is derived from (1) after normalizing with $(g_m/I_d)^2$.

Nevertheless, this method is obviously sensitive to the I_d/g_m factor, which in turn is influenced by the presence of

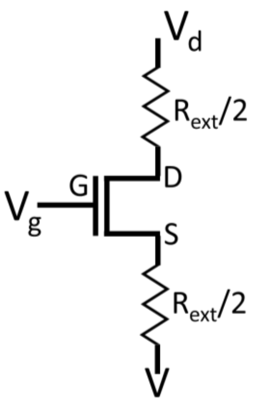

Fig. 1. Experimental set-up for monitoring the R_{SD} influence.

R_{SD}. For this reason, it is rather questionable whether the extraction of Ω by this established method is reliable. In order to monitor how the increase of R_{SD} can impact the extraction of Ω, we repeated the same LFN measurements on the same FinFET device for various combinations of externally connected resistors, R_{ext}, at both the drain ($R_{ext}/2$) and source ($R_{ext}/2$) terminals. The setup schematic is shown in Fig. 1.

The device under study is a n-channel FinFET fabricated at IMEC-Leuven, with number of fins N_{fin} = 22 nm, fin height H_{fin} = 26 nm, channel length L = 28 nm and fin width W_{fin} = 4.5 nm. The LFN measurements were performed using the programmable bias point probe system NOISYS7 [9], combined with a semi-auto 300 mm Cascade Micro Tech probe station. The simulations were performed using the FlexPDE [10] solver and the Python Spyder [11] platform.

III. Results And Discussion

Measurements of static $I_d(V_g)$ transfer characteristics were performed in linear region (V_d =30 mV) for different R_{ext} values. As shown in Fig. 2, there is a significant drain current degradation with R_{ext} in strong inversion.

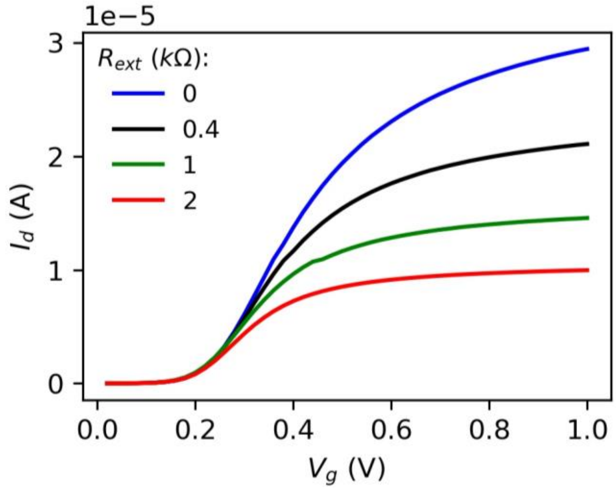

Fig. 2. Drain current versus gate voltage characteristics for various values of external resistance, R_{ext}.

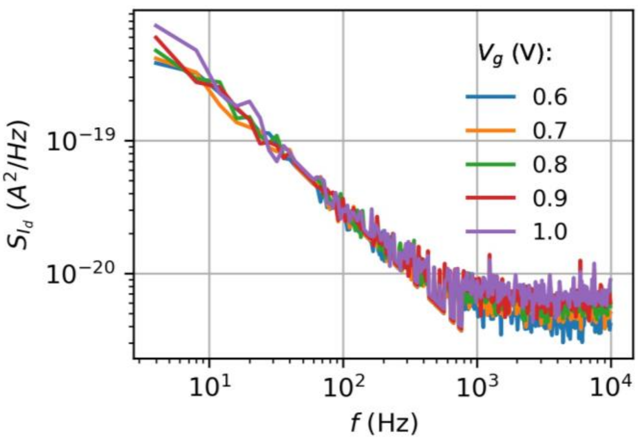

Fig. 3. Drain current noise power spectral density versus frequency for zero external resistance, R_{ext}=0 Ω at various gate bias values in strong inversion.

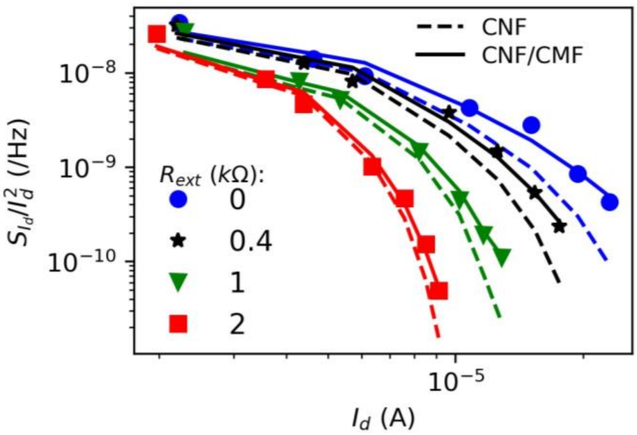

Fig. 4. Normalized drain current noise vs drain current along with the CNF and CNF/CMF fitting models for the different external resistance values, R_{ext}.

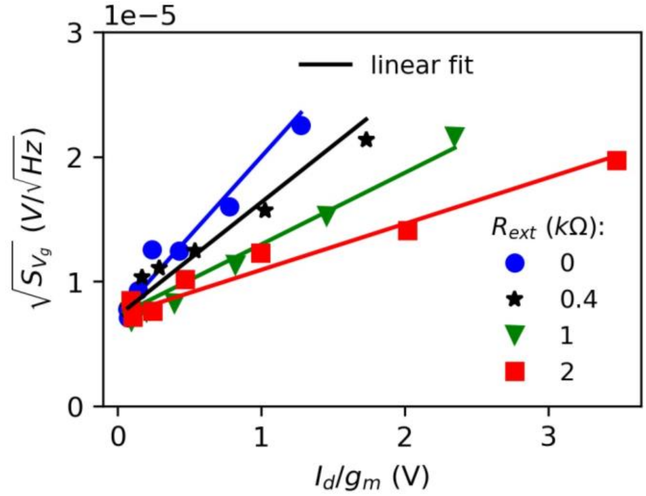

Fig. 5. Square root of input-referred noise, $\sqrt{S_{Vg}}$, versus the ratio of drain current and transconductance, I_d/g_m, for various external resistance values.

The next step is to study what is the impact of this phenomenon on the noise characterization. In Fig. 3, where the measured drain current noise spectral density is plotted versus frequency, one can observe a pure 1/f-like behavior, allowing us to apply the CNF/CMF model for the mean PSD value around 10 Hz.

Fig. 4 shows the plots of S_{Id}/I_d^2 around 10 Hz versus I_d for four different R_{ext} values along with the corresponding CNF/CMF model fit in the strong inversion region where the influence of R_{SD} takes place. The dotted lines represent the CNF/CMF model with Ω=0, to visualize how a high value of series resistance can make one think that there is no mobility fluctuations (CMF) contribution. Indeed, one can observe that as the series resistance increases, the experimental data approach the CNF model, eliminating almost completely the influence of CMF coefficient Ω in the maximum R_{ext} case (2 kΩ).

The same behavior can also be observed from the $\sqrt{S_{Vg}}$ vs I_d/g_m plot shown in Fig. 5, where we note that the slope of the characteristics changes with R_{ext}. This behavior with the series

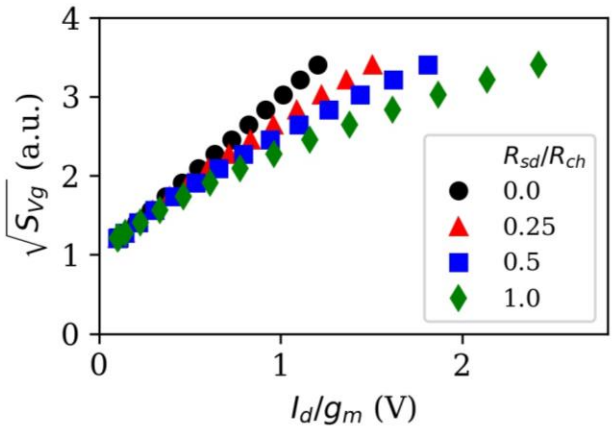

Fig. 6. Simulation results of square root of input-referred noise, $\sqrt{S_{Vg}}$, versus the ratio of drain current and transconductance, I_d/g_m for various R_{SD}/R_{CH} ratios.

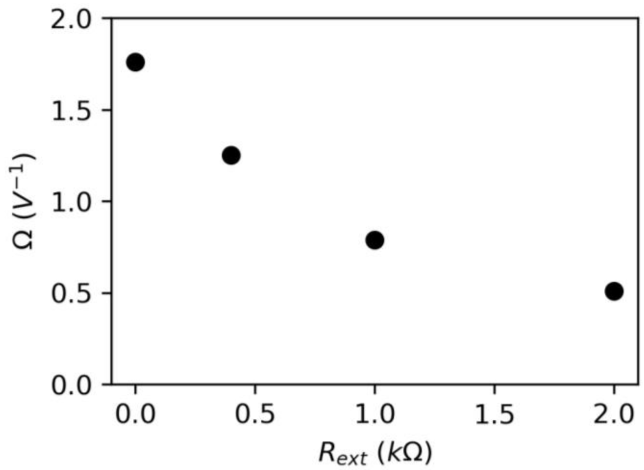

Fig. 7. Extracted CMF factor Ω versus the different R_{ext} values.

resistance was also confirmed by simulations, as shown in Fig. 6, where $R_{ch}=V_d/I_d$ is the channel resistance in ohmic region. This effect takes place because the presence of R_{ext} degrades g_m/I_d, thus leading to an increase of the I_d/g_m ratio, and shifts the experimental data points to the right, resulting to the unreliable extraction of the CMF factor Ω. Combining this finding with the fact that the intercept remains the same for all R_{ext} values and thus a constant value of S_{Vfb} can be extracted, we conclude that the diverging characteristics will lead in an underestimation of the Ω factor. By extracting S_{Vfb} from Fig. 4 and by taking a mean value of 5.24×10^{-11} V^2/Hz for S_{Vfb}, we pursued to the linear fit of (3) in Fig. 5 in order to calculate the Ω coefficient for the different R_{ext}. The dependence of this 'apparent' Ω on the presence of R_{ext} can be seen in Fig. 7. As expected, the extracted Ω factor is reduced with R_{ext}, revealing an underestimation due to the specific extraction process.

IV. New Extraction Methodology

To eliminate the impact of R_{SD} on the Ω extraction we can take advantage of the Y function, which is immune to the influence of series resistance [12] and is given by (4):

$$Y = I_d/\sqrt{g_m} \tag{4}$$

Fig. 8 depicts the Y-function plot for all the cases implying that the R_{ext} has been successfully compassed from the drain current. Henry *et al.* [13] published a new Y-function extraction method where I_d/g_m can be replaced as in (5):

$$\frac{I_d}{g_m} = n\frac{kT}{q} + \frac{Y}{\sqrt{\beta}} \tag{5}$$

where n is the transistor ideality factor and $\beta = V_d \mu_0 C_{ox} W/L$ its gain factor.

The combination of (4) and (5) considering that nkT/q is negligible in the strong inversion region results to (6):

$$\sqrt{S_{V_g}} = \sqrt{S_{V_{FB}}}\left[1 + \Omega\left(\frac{Y}{\sqrt{\beta}}\right)\right] \tag{6}$$

Therefore, if we plot $\sqrt{S_{Vg}}$ vs Y instead of I_d/g_m, as shown in Fig. 9, we can obtain a linear dependence which is not affected by the change in R_{ext}. This way a new, R_{SD}-independent value of Ω can be extracted, combining all groups of points. We extracted a value of Ω = 6.5 V^{-1}, much higher than the one extracted when R_{ext} = 0 Ω (1.75V^{-1}), revealing that the CMF contribution can indeed be completely overshadowed by the presence of a high series resistance value.

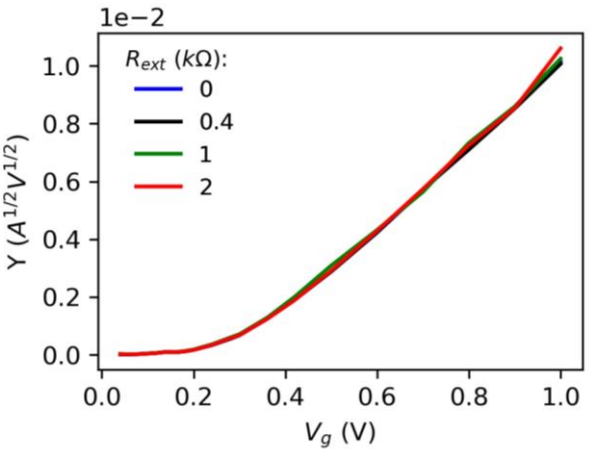

Fig. 8. Y-function versus gate voltage for the different external resistance values.

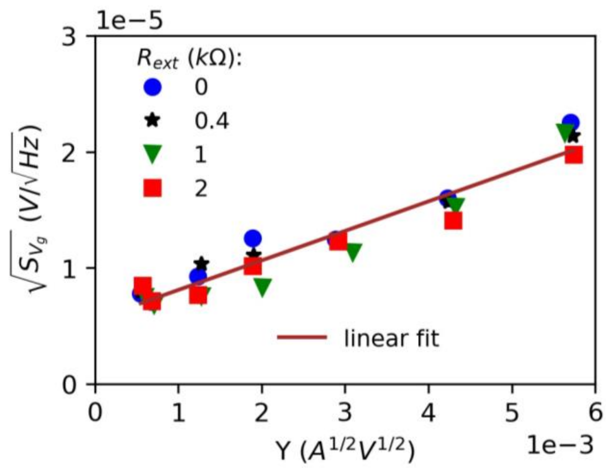

Fig. 9. Square root of input-referred noise versus Y-function for the different external resistance values, R_{ext}.

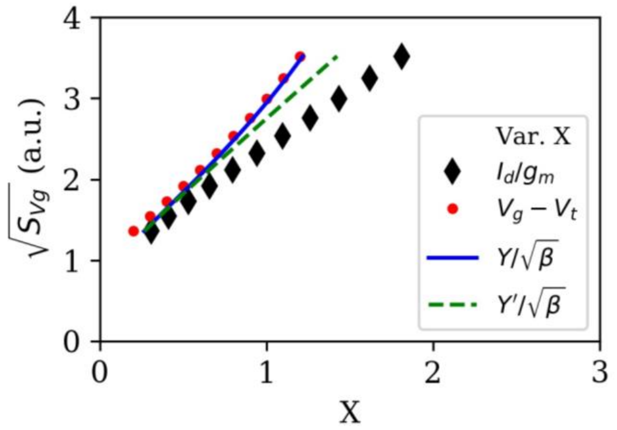

Fig. 10. Simulation results of square root of input-referred noise, $\sqrt{S_{Vg}}$, versus different X variables.

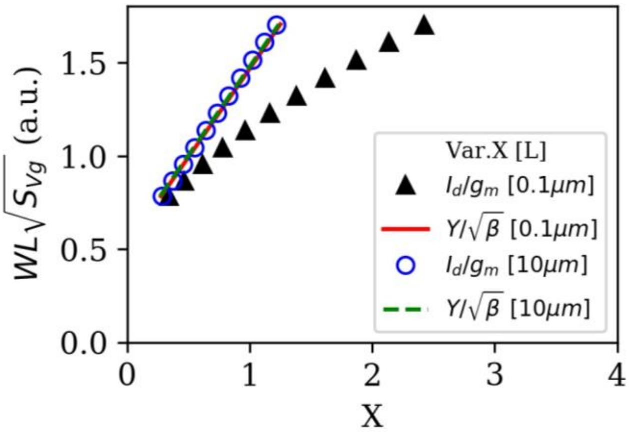

Fig. 11. Simulation results of normalized with area square root of input-referred noise, $WL\sqrt{S_{Vg}}$, versus different X variables.

It might be argued that by plotting $\sqrt{S_{Vg}}$ versus (V_g-V_t) would also give a straight line, but this is true when the mobility is degraded only due to the series resistance through the first order attenuation factor $\theta_1 \approx \beta^* R_{SD}/V_d$. However, in the possible presence of the second order mobility attenuation factor θ_2, the linearity with V_g-V_t is lost [14]. But if we use the Y-function expression (7) [12] that accounts for the influence of θ_2, a great linearity is achieved, as illustrated in Fig. 10, allowing for the proper extraction of Ω.

$$Y' = \sqrt{\frac{\beta}{1-\theta_2(V_g-V_t)^2}}(V_g - V_t) \qquad (7)$$

Moreover, concerning the channel length influence on this effect, since the impact of series resistance becomes negligible in long channel devices, we expect that both I_d/g_m and Y-function methods will give the same results. This was confirmed by simulations, where a 100 times longer channel was tested, for the same value of R_{SD} = 1 kΩ. As can be seen in Fig. 11, the series resistance affects significantly the L = 0.1µm parameter extraction, whereas for L = 10µm there is no R_{SD} influence on the extraction precision. Therefore, the Y-function method we propose is valid regardless the channel length.

V. Conclusion

The impact of R_{SD} on the extraction of noise parameters and especially on the Ω coefficient has been studied for FinFETs of 4.5 nm wide channel. It was found that the degradation of g_m/I_d due to the presence of R_{SD} results to the unreliable extraction of Ω and in high values of R_{SD} the mobility fluctuation due to charged traps can be heavily underestimated. To respond to this challenge, a new extraction methodology is proposed which utilizes the Y-function to successfully eliminate the R_{SD} influence.

Acknowledgment

The authors would like to acknowledge the Horizon 2020 ASCENT EU project (Access to European Nanoelectronics Network -Project no. 654384). They would also like to thank Thomas Chiarella and Jerome Mitard from IMEC-Leuven for their technical help and general support.

References

[1] G. Ghibaudo, O. Roux-dit-Buisson, and J. Brini, “Impact of Scaling Down on Low Frequency Noise in Silicon MOS Transistors,” *Phys. Status Solidi*, vol. 132, no. 2, pp. 501–507, Aug. 1992.

[2] D. M. Fleetwood, “1/f Noise and Defects in Microelectronic Materials and Devices,” *IEEE Trans. Nucl. Sci.*, vol. 62, no. 4, pp. 1462–1486, 2015.

[3] N. B. Lukyanchikova, M. V Petrichuk, N. P. Garbar, E. Simoen, and C. Claeys, “Non-trivial GR and 1/f noise generated in the p-Si layer of SOI and SOS MOSFETs near the inverted front or buried p-Si/SiO2 interface,” *Semicond. Sci. Technol.*, vol. 14, no. 9, pp. 775–783, 1999.

[4] C. G. Theodorou, N. Fasarakis, T. Hoffman, T. Chiarella, G. Ghibaudo, and C. A. A. Dimitriadis, “Flicker noise in n-channel nanoscale tri-gate fin-shaped field-effect transistors,” *Appl. Phys. Lett.*, vol. 101, no. 24, p. 243512, 2012.

[5] H. Achour *et al.*, “In depth static and low-frequency noise characterization of n-channel FinFETs on SOI substrates at cryogenic temperature,” *Solid. State. Electron.*, vol. 98, pp. 12–19, 2014.

[6] G. Ghibaudo, O. Roux, C. Nguyen-Duc, F. Balestra, and J. Brini, “Improved Analysis of Low Frequency Noise in Field-Effect MOS Transistors,” *Phys. Status Solidi*, vol. 124, no. 2, pp. 571–581, 1991.

[7] E. G. Ioannidis, C. A. Dimitriadis, S. Haendler, R. A. Bianchi, J. Jomaah, and G. Ghibaudo, “Improved analysis and modeling of low-frequency noise in nanoscale MOSFETs,” *Solid. State. Electron.*, vol. 76, pp. 54–59, 2012.

[8] E. G. Ioannidis, C. G. Theodorou, T. A. Karatsori, S. Haendler, C. A. Dimitriadis, and G. Ghibaudo, “Drain-Current Flicker Noise Modeling in nMOSFETs From a 14-nm FDSOI Technology,” *IEEE Trans. Electron Devices*, vol. 62, no. 5, pp. 1574–1579, 2015.

[9] J. A. Chroboczek, A. Szewczyk, and G. Piantino, “Low frequency noise point probe measurements on a wafer level using a novel programmable current amplifier,” in *Noise in Physical Systems and 1/F Fluctuations*, 2001, pp. 701–704.

[10] “Flex PDE.” [Online]. Available: https://www.pdesolutions.com/.

[11] “Spyder IDE.” [Online]. Available: https://www.spyder-ide.org/.

[12] D. Fleury, A. Cros, H. Brut, and G. Ghibaudo, “New Y-function-based methodology for accurate extraction of electrical parameters on nano-scaled MOSFETs,” *IEEE Int. Conf. Microelectron. Test Struct.*, pp. 160–165, 2008.

[13] J. B. Henry, Q. Rafhay, A. Cros, and G. Ghibaudo, “New Y-function based MOSFET parameter extraction method from weak to strong inversion range,” *Solid-State Electronics*. 2016.

[14] T. Boutchacha and G. Ghibaudo, “Improved modeling of low-frequency noise in MOSFETs - Focus on surface roughness effect and saturation region,” *IEEE Trans. Electron Devices*, vol. 58, no. 9, pp. 3156–3161, 2011.